NASA CONTRACTOR REPORT

AN EXPERIMENTAL INVESTIGATION OF VORTEX GENERATION IN A TURBULENT BOUNDARY LAYER UNDERGOING ADVERSE PRESSURE GRADIENT

by Victor Zakkay and Wladimiro Calarese

Prepared by
NEW YORK UNIVERSITY
University Heights, Bronx, N.Y. 10453
for Langley Research Center

NATIONAL AERONAUTICS AND SPACE ADMINISTRATION • WASHINGTON, D. C. • JUNE 1972

1. Report No.	2. Government Accession No.	3. Recipient's Catalog No.
NASA CR-2037		

4. Title and Subtitle	5. Report Date
AN EXPERIMENTAL INVESTIGATION OF VORTEX GENERATION IN A TURBULENT BOUNDARY LAYER UNDERGOING ADVERSE PRESSURE GRADIENT	June 1972
	6. Performing Organization Code

7. Author(s)	8. Performing Organization Report No.
Victor Zakkay and Wladimiro Calarese	N/A
	10. Work Unit No.

9. Performing Organization Name and Address	11. Contract or Grant No.
New York University School of Engineering and Science Daniel Guggenheim School of Aeronautics University Heights, Bronx, NY 10453	NGR-33-016-184
	13. Type of Report and Period Covered
12. Sponsoring Agency Name and Address National Aeronautics and Space Administration Washington, D.C. 20546	Contractor Report
	14. Sponsoring Agency Code

15. Supplementary Notes

16. Abstract

The investigation was undertaken to reveal the existence of streamwise vortices in nominally 2-dimensional boundary layers undergoing adverse pressure gradient. The free stream Mach number was $M_\infty = 5.75$, the wall to stagnation temperature ratio was $T_w/T_{t\infty} = 0.63$ and the Reynolds number based on free stream conditions was $R_e = 3.9 \times 10^7$/ft. The model consisted of an axisymmetric compression flare preceded by a cylindrical axially symmetric body. A natural turbulent boundary layer was established well ahead of the compression region. Boundary layer profiles of static pressure, pitot pressure, and stagnation temperature were taken at a surface station with a local inclination of 20^0. Profile measurements were obtained at various peripheral stations. The measurements revealed zero peripheral variations at the surface of the body and at the edge of the boundary layer. However, distinct wavy pressure variations were observed within the boundary layer profiles, indicating the existence of longitudinal vortex cells within the boundary layer.

17. Key Words (Suggested by Author(s))	18. Distribution Statement
vortex flow turbulent flow adverse pressure gradient	Unclassified - Unlimited

19. Security Classif. (of this report)	20. Security Classif. (of this page)	21. No. of Pages	22. Price*
Unclassified	Unclassified	42	$3.00

*For sale by the National Technical Information Service, Springfield, Virginia 22151

AN EXPERIMENTAL INVESTIGATION OF VORTEX GENERATION IN A TURBULENT BOUNDARY LAYER UNDERGOING ADVERSE PRESSURE GRADIENT*

by

Victor Zakkay† and Wladimiro Calarese††

SUMMARY AND INTRODUCTION

Previous boundary layer measurements along a concave wall have revealed a spanwise variation in velocity. The variation has been attributed to a system of vortices with axis in the streamwise direction[1]. These initial observations were made in a low speed turbulent boundary layer. At compressible speeds, evidence of these vortices has been observed in quasi two-dimensional flows in regions of separated flow reattachment[2,3]. However, well documented work along gradual adverse pressure gradient bodies did not reveal such variations[4,5].

Recent analysis of flows with adverse pressure gradient[6] indicates that some of the discrepancy between the analysis and some of the experimental work[5,7] is in part due to possible three-dimensional effects (such as the formation of Gorther vortices due to a concave curvature).

---

* The work reported herein was supported by the National Aeronautics & Space Administration under Grant NGR-33-016-184

† Professor of Aeronautics and Astronautics, New York University

†† Assistant Research Scientist, New York University

The present investigation was undertaken in order to determine the existence of such vortices utilizing the same apparatus used in Ref. 7. The free stream Mach number was $M_\infty = 5.75$, the wall to stagnation temperature ratio was $T_w/T_{t_\infty} = 0.63$ and the Reynolds number based on free stream conditions was $R_e = 3.9 \times 10^7/\text{ft}$. The model consisted of an axisymmetric compression flare preceded by a cylindrical axially symmetric body. A natural turbulent boundary layer was established well ahead of the compression region. Boundary layer profiles of static pressure, pitot pressure, and stagnation temperature were taken at a surface station with a local inclination of 20°. Profile measurements were obtained at various peripheral stations. The measurements revealed zero peripheral variations at the surface of the body and at the edge of the boundary layer. However, distinct wavy pressure variations were observed within the boundary layer profiles.

LIST OF SYMBOLS

M	Mach number
p	Pressure
Re	Reynolds number
S_1	Streamwise distance from the leading edge of the model to beginning of flare
S'	Streamwise distance measured from beginning of flare
S	$S_1 + S'$
T	Temperature
u	Velocity in streamwise direction
x	Axial direction
y	Direction normal to the body surface
δ	Boundary layer thickness
η	Local surface inclination with respect to body axis
φ	Peripheral angle

Subscripts

e	Conditions external to the boundary layer
s	Static conditions
T	Stagnation conditions
2	Behind normal shock
∞	Free stream conditions

I. EXPERIMENTAL APPARATUS

The tests were performed in the New York University Mach 6 high Reynolds number facility. The facility consists of a 2200 psia air supply; a capacity heater capable of delivering 900°R air with a mass flux of up to 60 lbs/sec, and capable of supplying nominally constant stagnation temperature flows for up to 40 sec. of running time. The test section is 1 ft. in diameter and consists of a uniform flow 9 in. in diameter and 3 ft. in length (Fig. 1). The free stream Mach number was approximately 5.75. For all tests, the stagnation temperature was about 860°R, and the stagnation pressures varied between 1860 and 1900 psia. The Reynolds number was of the order of 3.9×10^7/ft. The model consisted of an axisymmetric compression surface, described by a fourth order polynomial, blended into a 42° conical surface 6 in. in length, with a base diameter of 7.96 in. The compression model is attached to a fore-body consisting of an open sharp edge right-circular cylinder 29.2 in. long and 4.62 in. in diameter (Figs. 2-3). The coordinates of the flare are given in Table 1. The model is placed coaxially within the tunnel centerline (Fig. 4). The tests were performed at a surface station with 20° local inclination, $\eta = 20^\circ$, and repeated every 5° in the peripheral direction from $\varphi = 0^\circ$ to $\varphi = 40^\circ$. The compression flare was equipped with 30 pressure orifices. To obtain measurements of static and pitot pressures, and stagnation temperatures throughout the boundary layer, single probes were used (Fig. 5). Special care was taken in placing the probes at exactly $\eta = 20^\circ$, when going from one peripheral station to the next, and with the right inclination in order to traverse the boundary layer normal to the body. The static pressure probes used for the present ex-

periment had a flat tip faired into a 0.040 in. hypodermic needle. Lateral orifices located 10 to 15 probe diameters downstream were drilled in order to decrease their sensitivity to yaw angles. The pitot pressure probes consisted of a hypodermic needle of 0.04 in. diameter flattened at the tip with a thickness of 0.006 in. and an opening of 0.002 in. An unshielded, open-tip chromel-alumel thermocouple was used to measure the stagnation temperature throughout the boundary layer.

II. DISCUSSION OF MEASUREMENTS

The pressure and total temperature measurements are presented in Tables 2-11 in tabulated form. For all tests a turbulent boundary layer was obtained and no separation was observed on the compression flare. All the measurements were taken at one location, i.e. $\eta = 20^{\circ}$, and were repeated in the peripheral direction, from $\varphi = 0^{\circ}$ to $\varphi = 40^{\circ}$. The static and pitot pressure profiles are shown in(Fig. 6-14). The wall pressure is that obtained from the pressure taps located on the surface of the compression flare. The static pressure decreases in the y direction due to the normal pressure gradient; the pitot pressure experiences severe losses in the low density region of the boundary layer near the wall. In this region, at y = 0.02 in., the pitot pressure has a higher value than expected. This is due to probe interference, as reported by Hoydysh and Zakkay[7]. The normal shock ahead of the probe interacts with the boundary layer causing local separation.

Both static and pitot pressure are plotted as functions of the peripheral angle φ in (Figs. 15-16). At the wall the values are constant but, traversing away from the wall, they have a wavy pattern in the peripheral direction with an amplitide of about four times the boundary layer thickness. This behavior is present up to the edge of the boundary layer, approximately 0.20 in. in thickness and vanishes outside the boundary layer. At 0.35 in. away from the wall in the normal direction, the pressure goes back to constant values in the peripheral direction.

The total temperature profiles are shown in (Fig. 17). The total temperature recovers very quickly in the normal direction and attains 95% of its free stream value in less than 0.03 in.; its peripheral distribution is

almost constant at any distance from the wall (Fig. 18).

The Mach number and velocity profiles are plotted respectively in (Fig. 19 and Fig. 20). The velocity profiles are the typical turbulent profiles bent in the central region of the boundary layer because of the presence of an adverse pressure gradient; the peripheral distribution shows a slight perturbation which vanishes at the edge of the boundary (Fig. 21). The Mach number distribution shows the same peripheral perturbation as the pressure distribution up to the edge of the boundary layer.

CONCLUSIONS

An experimental investigation has been undertaken to ascertain the possible presence of vortices in a hypersonic turbulent boundary layer over an axisymmetric configuration in presence of adverse pressure gradient. Experimental data obtained at one longitudinal station in the peripheral direction has been tabulated and plotted.

The data shows large pressure differential in the boundary layer away from the wall that implies the incipient formation of a swirling flow. This peripheral variation vanishes outside the boundary layer where the axisymmetric flow properties are restored. Nothing can be said as to the starting region of the swirling flow and the further developments beyond the location where the measurements were taken since no measurements were performed in that region.

It is felt that additional measurements are necessary to establish the behavior of the flow over the compression flare and to determine the initial generation of the vortices.

Since this work has been probing in nature, it would be of significant interest in establishing the region where the vortices are generated, and their development along the compression surface. Other techniques for probing the fluctuation intensity such as with a laser dopplemeter, or other measuring techniques may be necessary in order to establish the wave pattern of the vortices.

REFERENCES

1. Tani, Itiro, "Production of Longitudinal Vortices in the Boundary Layer Along a Concave Wall," Journal of Geophysical Research, Vol. 67, No. 8, July 1962, pp. 3075-3080.

2. Persen, Leif, N., "Investigation of Streamwise Vortex System Generated in Certain Classes of Curved Flow," Part I, ARL-68-0134, July 1968.

3. Ginoux, Jean, J., "Streamwise Vortices in Reattaching High-Speed Flows," A suggested approach, AIAA Journal, Vol. 9, No. 4, December 15, 1970, pp. 759-760.

4. Thomann, G., "Heat Transfer in a Turbulent Boundary Layer with a Pressure Gradient Normal to the Flow," The Aeronautical Research Institute of Sweden, Meddelande 113, Report 113, Stockholm, July 1967.

5. McLafferty, George H. and Barber, Robert, E., "Turbulent Boundary Layer Characteristics in Supersonic Streams Having Adverse Pressure Gradients," United Aircraft Corporation, Report No. R-1285, September 1959.

6. Bushnell, D.M. and Alston, D.W., "On The Calculation of Compressible Adverse Pressure Gradient Turbulent Boundary Layers," proposed AIAA TN, NASA Langley Research Center, Hampton, Virginia.

7. Hoydysh, Walter, G., and Zakkay, Victor, "An Experumental Investigation of Hypersonic Turbulent Boundary Layers in Adverse Pressure Gradient," AIAA Paper No. 68-44.

x (in.)	R (in.)	η (deg.)	s (in.)
0.0	2.310	0.0	0.0
0.4	2.319	2.0	0.400
0.8	2.339	3.5	0.800
1.2	2.367	4.9	1.201
1.6	2.410	6.5	1.603
2.0	2.465	8.5	2.006
2.4	2.527	10.0	2.411
2.8	2.600	11.0	2.818
3.2	2.686	12.0	3.228
3.6	2.782	14.2	3.642
4.0	2.890	16.7	4.061
4.4	3.021	21.4	4.486
4.8	3.195	25.0	4.919
5.2	3.394	28.2	5.365
5.6	3.634	34.6	5.834
6.0	3.930	42.0	6.355

Table 1. Body Coordinates of Flare.

TAP NO.	x (in.)	η (Deg.)	ϕ (Deg.)	p_s (psia)
1	0.4	2°	0°	1.45
2	0.78	3.45°	5°	1.6
3	1.18	4.8	10°	1.93
4	1.63	6.55	15°	2.5
5	2.00	8.5	20°	2.7
6	2.40	10.0	25°	3.15
7	2.87	11.25	30°	3.8
8	3.30	13.0	35°	5.55
9	3.75	15°	40	8.0
10	4.25	19.25	50	12.7
11	4.50	22.5	60	15.1
12	4.60	23.5	70	16.95
13	5.00	26.5	80	22.9
14	4.35	20°	0°	14.6
15	4.35	20°	5°	14.6
16	4.35	20°	10°	15.0
17	4.35	20°	15°	15.0
18	4.35	20°	20°	14.5
19	4.35	20°	25°	14.5
20	4.35	20°	30°	14.7
21	4.35	20°	35°	14.7
22	4.35	20°	40°	14.7

Table.2. Surface Pressure Distribution .

$\phi = 0^\circ$ $p_{T_\infty} =$ 1900 psia (FOR STATIC PRESSURE)

$\eta = 20^\circ$; $p_{T_\infty} =$ 1900 psia (FOR PITOT PRESSURE); $T_{T_\infty} = 860^\circ R$

y	p_s	p_{T_2}	T_T	p_{T_∞}	y	p_s	p_{T_2}	T_T	p_{T_∞}
0	14.7	82	535	1865	.24	6.4	165	806	1785
.01	14.6	80	741	1862	.25	5.8	158	805	1780
.02	14.3	82	763.5	1858	.26	5.3	146	803	1775
.03	14.1	120	780	1855	.27	4.7	135	800	1770
.04	13.8	138	785	1850	.28	4.1	127	797	1767
.05	13.5	130	787	1848	.29	3.7	114	794	1764
.06	13.2	130	788	1845	.30	3.3	108	791	1760
.07	12.9	132	790	1842	.31	2.8	80	788	1755
.08	12.6	140	791	1839	.32	2.2	64	785	1750
.09	12.3	145	794	1835	.33	1.9	59	783	1745
.10	12.0	150	795	1832	.34	1.7	59	782	1740
.11	11.7	152	798	1830	.35	1.5		780.5	
.12	11.4	158	800	1827	.36	1.45		779	
.13	11.2	162	803	1824	.37	1.35		777	
.14	10.9	168	805	1820	.38				
.15	10.6	174	807	1817	.39				
.16	10.3	180	809	1816	.40				
.17	10.0	184	811	1810	.41				
.18	9.6	186	813	1805	.42				
.19	9.1	186	814	1800	.43				
.20	8.6	183	814	1797	.44				
.21	8.1	180	813	1795	.45				
.22	7.4	175	810	1795	.46				
.23	6.9	170	808	1790	.47				

Table 3. Tabulated Data for Pressure and Temperature.

$\phi = 5^0$ $p_{T_\infty} =$ 1890 psia (FOR STATIC PRESSURE)

$\eta = 20^\circ$; $p_{T_\infty} =$ 1850 psia (FOR PITOT PRESSURE); $T_{T_\infty} = 860^\circ R$

y	p_s	p_{T_2}	T_T	p_{T_∞}	y	p_s	p_{T_2}	T_T	p_{T_∞}
0	14.8	92	535	1830	.24	6.3	162	818	1754
.01	14.6	98	743	1828	.25	5.7	154	817	1750
.02	14.4	125	764	1826	.26	5.25	144	817	1748
.03	14.0	125	779	1824	.27	4.8	139	816	1745
.04	13.8	125	785	1820	.28	4.2	130	815	1742
.05	13.4	128	787	1815	.29	3.8	116	814	1740
.06	13.7	128	789	1810	.30	3.3	85	811	1735
.07	12.70	132	791	1805	.31	2.9	72	807	1730
.08	12.4	138	793	1802	.32	2.4	60	803	1725
.09	12.2	140	796	1800	.33	1.9	59	800	1720
.10	11.8	146	799	1798	.34	1.7		798	
.11	11.5	152	802	1796	.35	1.5		797	
.12	11.2	160	805	1792	.36	1.45		795	
.13	10.9	167	809	1789	.37	1.35		795	
.14	10.6	172	812	1785	.38				
.15	10.2	178	815	1780	.39				
.16	9.8	180	818	1775	.40				
.17	9.4	185	820	1774	.41				
.18	9.05	188	822	1772	.42				
.19	8.7	185	822	1770	.43				
.20	8.1	182	822	1766	.44				
.21	7.65	180	822	1762	.45				
.22	7.3	174	820	1760	.46				
.23	6.7	170	820	1757	.47				

Table 4. Tabulated Data for Pressure and Temperature.

$\phi = 10^{\circ}$ $p_{T_\infty} =$ 1880 psia (FOR STATIC PRESSURE)

$\eta = 20^{\circ}$; $p_{T_\infty} =$ 1870 psia (FOR PITOT PRESSURE); $T_{T_\infty} = 868^{\circ}R$

y	p_s	p_{T_2}	T_T	p_{T_∞}	y	p_s	p_{T_2}	T_T	p_{T_∞}
0	14.8	92	535	1840	.24	5.2	158	811	1763
.01	14.6	98	759	1838	.25	4.9	148	810	1760
.02	14.4	130	762	1835	.26	4.6	142	810	1757
.03	14.0	129	773	1833	.27	4.0	130	809	1753
.04	13.8	130	785	1830	.28	3.7	120	807	1750
.05	13.4	130	792	1825	.29	3.3	108	803	1747
.06	13.1	134	795	1820	.30	3.0	86	798	1745
.07	12.70	140	797	1815	.31	2.5	65	795	1740
.08	12.40	144	800	1811	.32	2.2	60	792	1735
.09	12.00	148	803	1809	.33	1.7	59	790	1730
.10	11.60	152	804	1807	.34	1.5		787	
.11	11.10	157	805	1805	.35	1.45		786	
.12	10.70	160	807	1800	.36	1.35		785	
.13	10.40	168	810	1797	.37	1.25		784	
.14	10.00	172	813	1793	.38				
.15	9.5	180	815	1790	.39				
.16	9.2	183	818	1785	.40				
.17	8.7	186	819	1783	.41				
.18	8.3	186	821	1780	.42				
.19	7.8	185	821	1778	.43				
.20	7.30	181	821	1775	.44				
.21	6.8	175	819	1770	.45				
.22	6.3	171	817	1768	.46				
.23	5.7	165	813	1765	.47				

Table 5. Tabulated Data for Pressure and Temperature.

$\phi = 15^\circ$ $p_{T_\infty} =$ 1860 psia (FOR STATIC PRESSURE)

$\eta = 20^\circ$; $p_{T_\infty} =$ 1900 psia (FOR PITOT PRESSURE); $T_{T_\infty} = 868^\circ R$

y	p_s	p_{T_2}	T_T	p_{T_∞}	y	p_s	p_{T_2}	T_T	p_{T_∞}
0	14.8	95	535	1865	.24	6.0	163	810	1785
.01	14.6	100	760	1862	.25	5.55	152	810	1780
.02	14.4	138	759	1858	.26	4.95	145	810	1775
.03	14.2	138	768	1855	.27	4.4	133	809	1770
.04	14.0	135	782	1850	.28	3.7	123	808	1767
.05	13.6	140	787	1848	.29	3.2	101	806	1764
.06	13.3	145	792	1845	.30	2.8	80	803	1760
.07	12.9	150	795	1842	.31	2.4	66	798	1755
.08	12.6	153	797	1839	.32	2.1	60	795	1750
.09	12.1	160	798	1835	.33	1.6	60	793	1745
.10	11.8	170	800	1832	.34	1.5		790	1740
.11	11.6	176	801	1830	.35	1.4		787	
.12	11.1	178	803	1827	.36	1.35		787	
.13	10.8	180	805	1824	.37	1.25		785	
.14	10.6	186	807	1820	.38				
.15	10.2	190	810	1817	.39				
.16	9.75	190	813	1816	.40				
.17	9.2	193	816	1810	.41				
.18	8.8	193	816	1805	.42				
.19	8.4	189	816	1800	.43				
.20	8.0	185	815	1797	.44				
.21	7.5	180	813	1795	.45				
.22	7.0	174	812	1795	.46				
.23	6.5	170	812	1790	.47				

Table 6. Tabulated Data for Pressure and Temperature.

$\phi = 20^{\circ}$ $p_{T_\infty} =$ 1900 psia (FOR STATIC PRESSURE)

$\eta =$ 20°; $p_{T_\infty} =$ 1900 psia (FOR PITOT PRESSURE); $T_{T_\infty} = 860^{\circ}R$

y	p_s	p_{T_2}	T_T	p_{T_∞}	y	p_s	p_{T_2}	T_T	p_{T_∞}
0	14.7	80	535	1865	.24	7.4	160	800	1785
.01	14.6	90	753	1862	.25	6.8	152	800	1780
.02	14.3	145	752	1858	.26	6.1	140	800	1775
.03	14.1	140	753	1855	.27	5.5	128	798	1770
.04	13.8	140	766	1850	.28	5.0	110	795	1767
.05	13.5	140	775	1848	.29	4.2	83	793	1764
.06	13.2	140	780	1845	.30	3.5	68	792	1760
.07	12.9	143	782	1842	.31	3.0	61	789	1755
.08	12.6	150	783	1839	.32	2.5	60	785	1750
.09	12.3	155	785	1835	.33	2.1		783	1745
.10	12.1	164	786	1832	.34	1.8		781	1740
.11	11.8	166	788	1830	.35	1.6		778	
.12	11.7	174	793	1827	.36	1.5		778	
.13	11.6	178	796	1824	.37	1.35		777	
.14	11.3	180	798	1820	.38				
.15	10.9	186	800	1817	.39				
.16	10.6	192	803	1816	.40				
.17	10.3	192	804	1810	.41				
.18	9.9	191	805	1805	.42				
.19	9.6	189	805	1800	.43				
.20	9.2	185	804	1797	.44				
.21	8.8	180	804	1795	.45				
.22	8.3	173	804	1795	.46				
.23	7.8	167	801	1790	.47				

Table 7. Tabulated Data for Pressure and Temperature.

$\phi = 25^\circ$

$P_{T_\infty} =$ 1890 psia (FOR STATIC PRESSURE)

$\eta = 20^\circ$; $P_{T_\infty} =$ 1860 psia (FOR PITOT PRESSURE); $T_{T_\infty} = 858^\circ R$

y	P_s	P_{T_2}	T_T	P_{T_∞}	y	P_s	P_{T_2}	T_T	P_{T_∞}
0	14.8	80	535	1835	.24	5.2	154	785	1758
.01	14.6	90	760	1832	.25	4.7	145	784	1755
.02	14.2	145	757	1830	.26	4.2	134	782	1752
.03	13.8	140	760	1828	.27	3.8	121	781	1748
.04	13.4	140	770	1826	.28	3.5	97	780	1745
.05	13.1	140	774	1820	.29	3.2	80	779	1742
.06	12.7	140	782	1815	.30	2.8	65	778	1740
.07	12.4	145	785	1810	.31	2.5	60	777	1735
.08	12.0	152	785	1806	.32	2.2	59	776	1730
.09	11.6	156	785	1804	.33	1.9		774	
.10	11.5	162	787	1802	.34	1.8		772	
.11	10.75	165	789	1800	.35	1.6		770	
.12	10.4	174	791	1795	.36	1.5		769	
.13	9.8	177	796	1792	.37	1.35			
.14	9.5	180	800	1788	.38				
.15	9.1	185	801	1784	.39				
.16	8.7	190	803	1780	.40				
.17	8.2	190	803	1778	.41				
.18	7.8	190	800	1776	.42				
.19	7.25	185	797	1773	.43				
.20	6.95	182	793	1770	.44				
.21	6.5	177	791	1765	.45				
.22	6.0	170	788	1763	.46				
.23	5.6	162	787	1760	.47				

Table 8. Tabulated Data for Pressure and Temperature.

$\phi = 30^\circ$ $p_{T_\infty} =$ 1900 psia (FOR STATIC PRESSURE)

$\eta = 20^\circ$; $p_{T_\infty} =$ 1880 psia (FOR PITOT PRESSURE); $T_{T_\infty} = 860^\circ R$

y	p_s	p_{T_2}	T_T	p_{T_∞}	y	p_s	p_{T_2}	T_T	p_{T_∞}
0	14.8	80	535	1840	.24	4.7	155	793	1763
.01	14.7	90	770	1838	.25	4.25	145	793	1760
.02	14.6	100	768	1835	.26	3.9	132	793	1757
.03	14.4	140	778	1833	.27	3.4	120	793	1753
.04	14.0	140	781	1830	.28	3.15	100	793	1750
.05	13.5	145	785	1825	.29	2.8	75	793	1747
.06	13.6	145	790	1820	.30	2.5	70	792	1745
.07	12.8	148	792	1815	.31	2.3	61	790	1740
.08	12.4	152	794	1811	.32	2.0	59	790	1735
.09	12.0	158	795	1809	.33	1.8		788	1730
.10	11.6	165	797	1807	.34	1.6		787	
.11	11.0	170	800	1805	.35	1.4		786	
.12	10.7	175	801	1800	.36	1.35		785	
.13	10.2	182	802	1797	.37	1.35			
.14	9.7	187	802	1793	.38				
.15	9.2	190	801	1790	.39				
.16	8.75	193	800	1785	.40				
.17	8.25	193	799	1783	.41				
.18	7.7	193	798	1780	.42				
.19	7.1	188	797	1778	.43				
.20	6.7	182	797	1775	.44				
.21	6.1	178	795	1770	.45				
.22	5.7	170	795	1768	.46				
.23	5.15	162	793	1765	.47				

Table 9. Tabulated Data for Pressure and Temperature.

$\phi = 35^{\circ}$ $p_{T_\infty} = 1900$ psia (FOR STATIC PRESSURE)

$\eta = 20^{\circ}$; $p_{T_\infty} = 1870$ (FOR PITOT PRESSURE); $T_{T_\infty} = 860^{\circ}R$

y	p_s	p_{T_2}	T_T	p_{T_∞}	y	p_s	p_{T_2}	T_T	p_{T_∞}
0	14.8	90	535	1840	.24	4.5	141	800	1763
.01	14.6	100	768	1838	.25	4.0	130	800	1760
.02	14.4	142	770	1835	.26	3.7	114	800	1757
.03	14.0	142	773	1833	.27	3.4	91	799	1753
.04	13.5	147	785	1830	.28	3.0	66	798	1750
.05	13.2	149	790	1825	.29	2.7	62	797	1747
.06	12.8	152	792	1820	.30	2.4	60	795	1745
.07	12.4	155	795	1815	.31	2.1	59	792	1740
.08	12.0	163	795	1811	.32	1.8		789	1735
.09	12.0	170	795	1809	.33	1.6		786	1730
.10	11.7	172	795	1807	.34	1.5		784	
.11	11.2	178	795	1805	.35	1.3		781	
.12	10.9	183	795	1800	.36	1.25		780	
.13	10.4	186	795	1797	.37	1.25		779	
.14	9.75	191	797	1793	.38				
.15	9.3	194	798	1790	.39				
.16	8.75	191	800	1785	.40				
.17	8.25	189	803	1783	.41				
.18	7.60	183	804	1780	.42				
.19	7.0	178	803	1778	.43				
.20	6.3	172	803	1775	.44				
.21	5.9	166	803	1770	.45				
.22	5.3	158	803	1768	.46				
.23	4.9	150	803	1765	.47				

Table 10. Tabulated Data for Pressure and Temperature.

$\phi = 40^\circ$ $p_{T_\infty} =$ 1900 psia (FOR STATIC PRESSURE)

$\eta = 20^\circ$; $p_{T_\infty} =$ 1850 psia (FOR PITOT PRESSURE); $T_{T\infty} = 850^\circ R$

y	p_s	p_{T_2}	T_T	p_{T_∞}	y	p_s	p_{T_2}	T_T	p_{T_∞}
0	14.8	80	535	1830	.24	5.0	135	776	1754
.01	14.6	95	752	1828	.25	4.5	125	773	1750
.02	14.4	130	764	1826	.26	4.1	110	771	1748
.03	14.0	140	764	1824	.27	3.7	80	770	1745
.04	13.7	135	764	1820	.28	3.3	64	770	1742
.05	13.5	138	762	1815	.29	3.0	61	770	1740
.06	13.2	140	762	1810	.30	2.7	58	769	1735
.07	12.8	145	768	1805	.31	2.4		768	1730
.08	12.4	150	777	1802	.32	2.1		767	1725
.09	12.0	155	795	1800	.33	1.8		767	1720
.10	11.5	160	795	1798	.34	1.7		766	
.11	11.0	168	795	1796	.35	1.5		766	
.12	10.5	173	795	1792	.36	1.45		766	
.13	10.2	180	793	1789	.37	1.4		765	
.14	9.8	187	792	1785	.38				
.15	9.3	192	790	1780	.39				
.16	8.9	190	787	1775	.40				
.17	8.5	187	785	1774	.41				
.18	7.95	182	784	1772	.42				
.19	7.3	178	784	1770	.43				
.20	6.9	174	781	1766	.44				
.21	6.4	169	780	1762	.45				
.22	5.9	160	778	1760	.46				
.23	5.5	148	777	1757	.47				

Table 11. Tabulated Data for Pressure and Temperature.

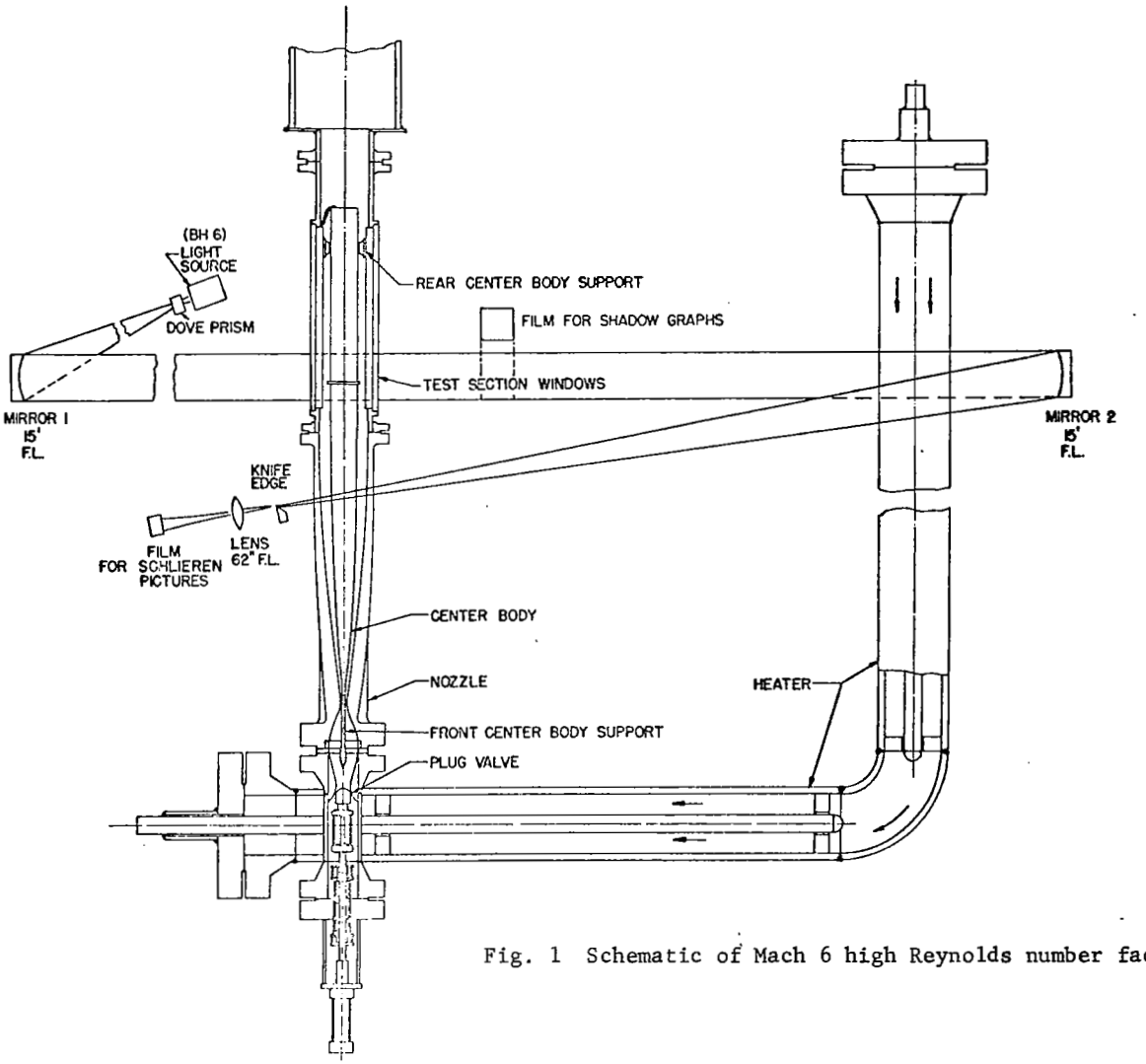

Fig. 1 Schematic of Mach 6 high Reynolds number facility

Fig. 2 Model forebody and flare

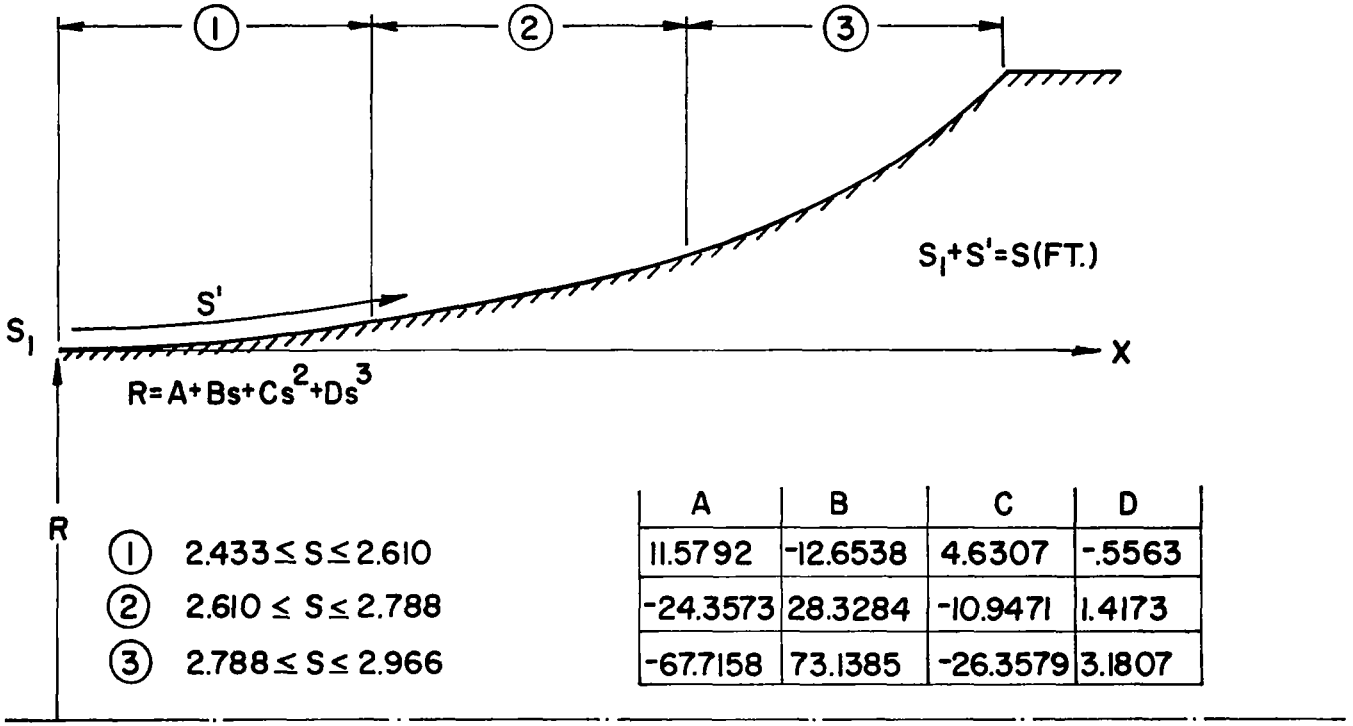

A	B	C	D
11.5792	-12.6538	4.6307	-.5563
-24.3573	28.3284	-10.9471	1.4173
-67.7158	73.1385	-26.3579	3.1807

Fig. 3 Geometry of flare

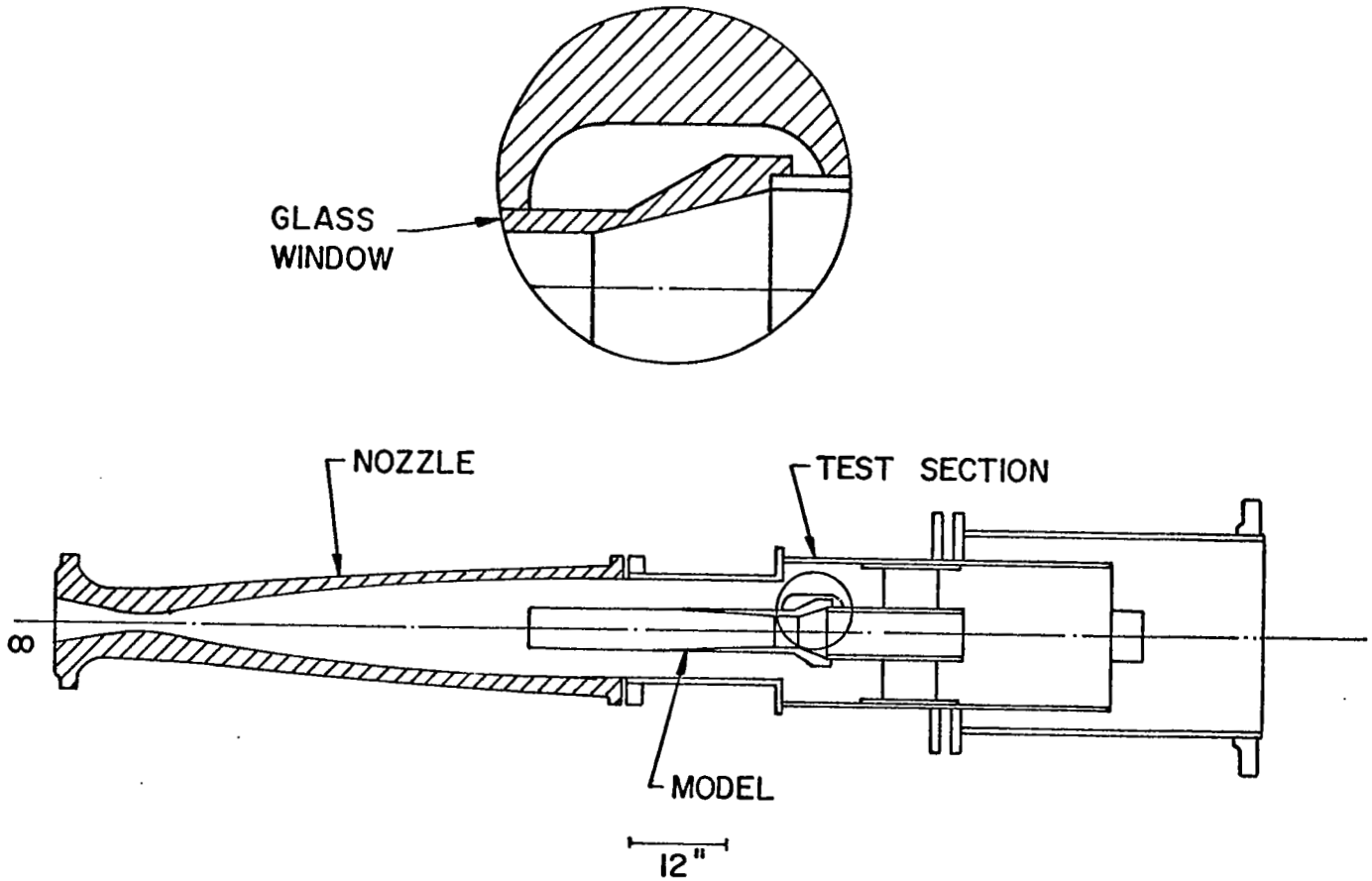

Fig. 4 Model test section assembly

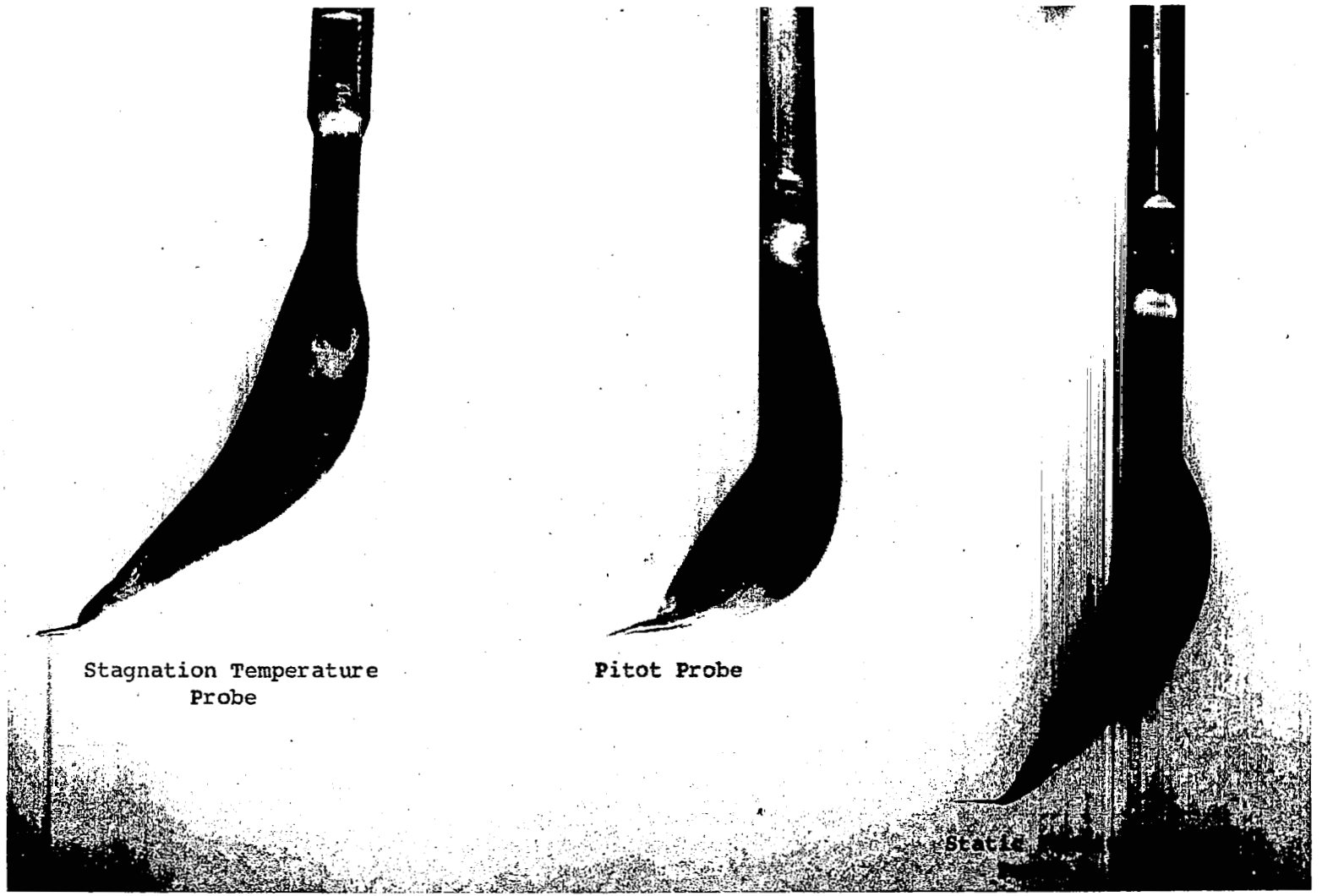

Fig. 5 Boundary layer probes

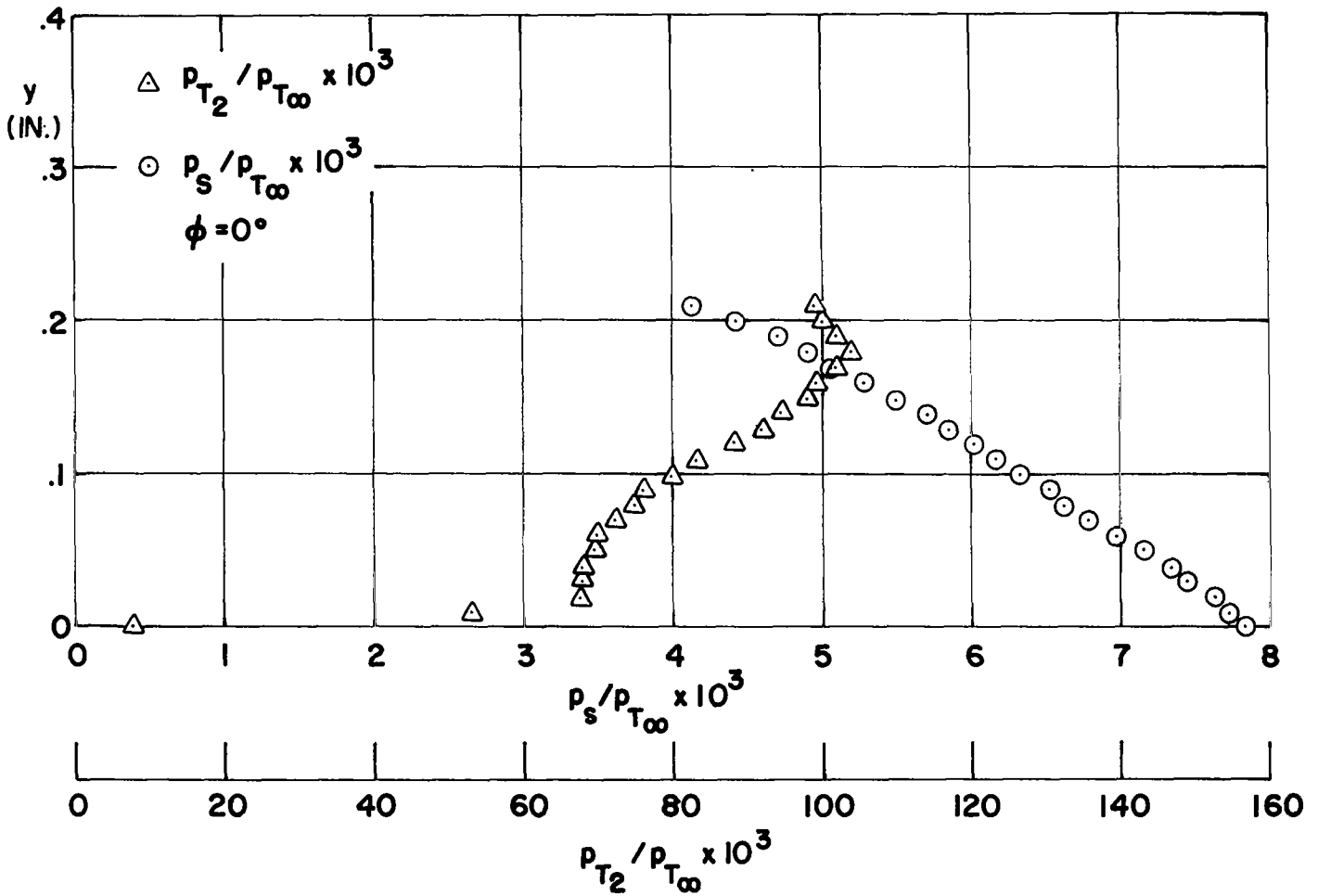

Fig. 6 Static and pitot pressure profiles

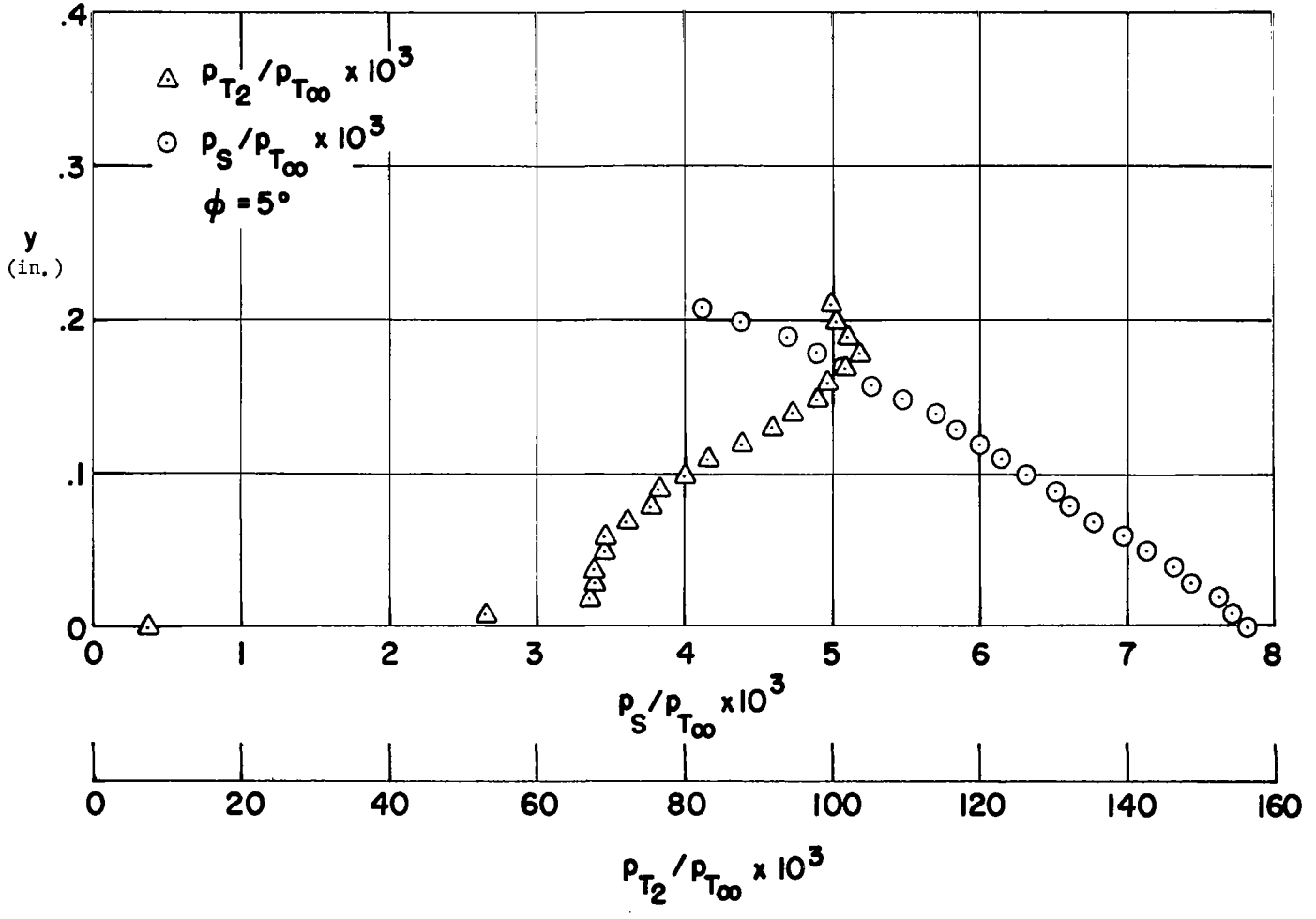

Fig. 7 Static and pitot pressure profiles

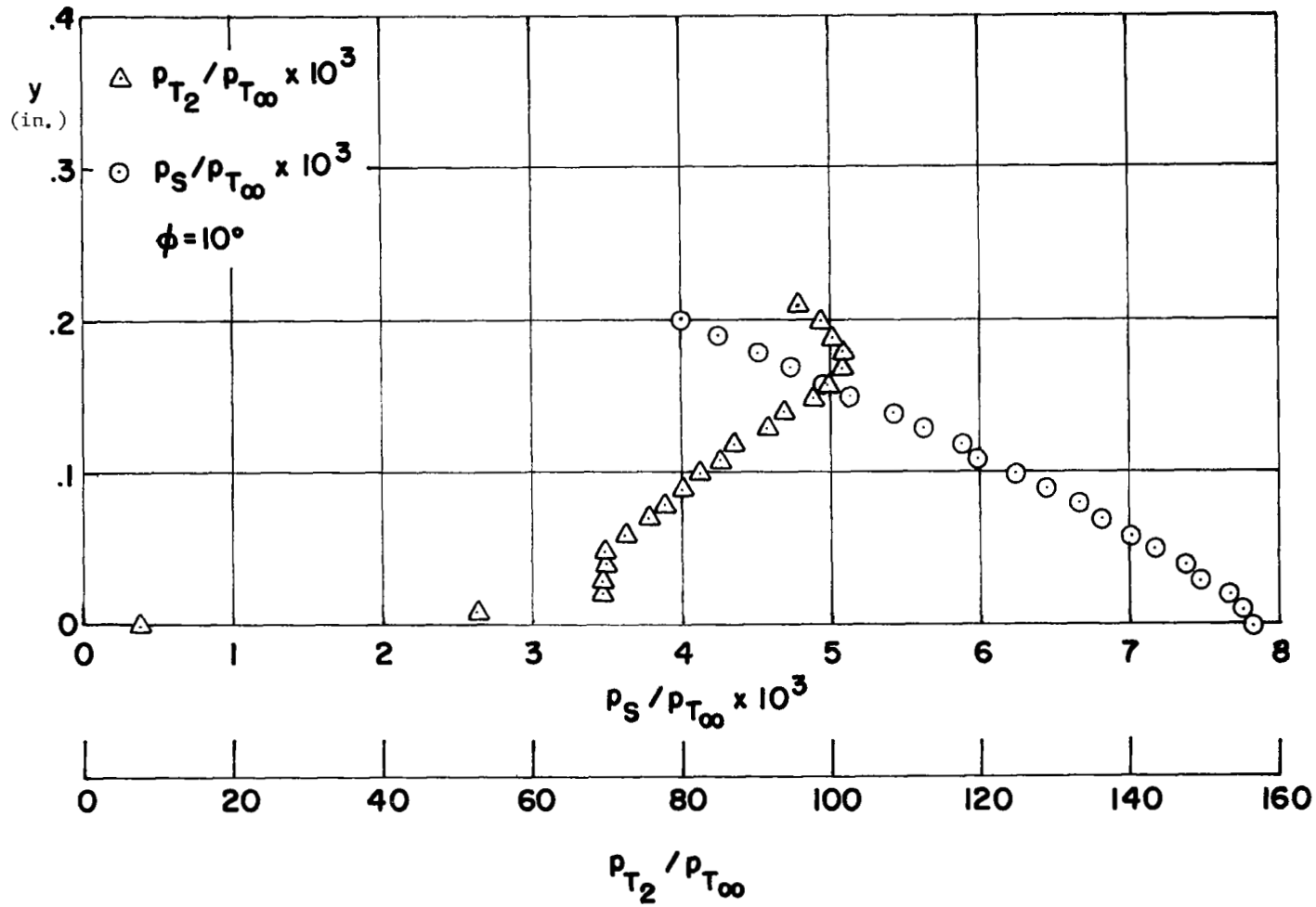

Fig. 8 Static and pitot pressure profiles

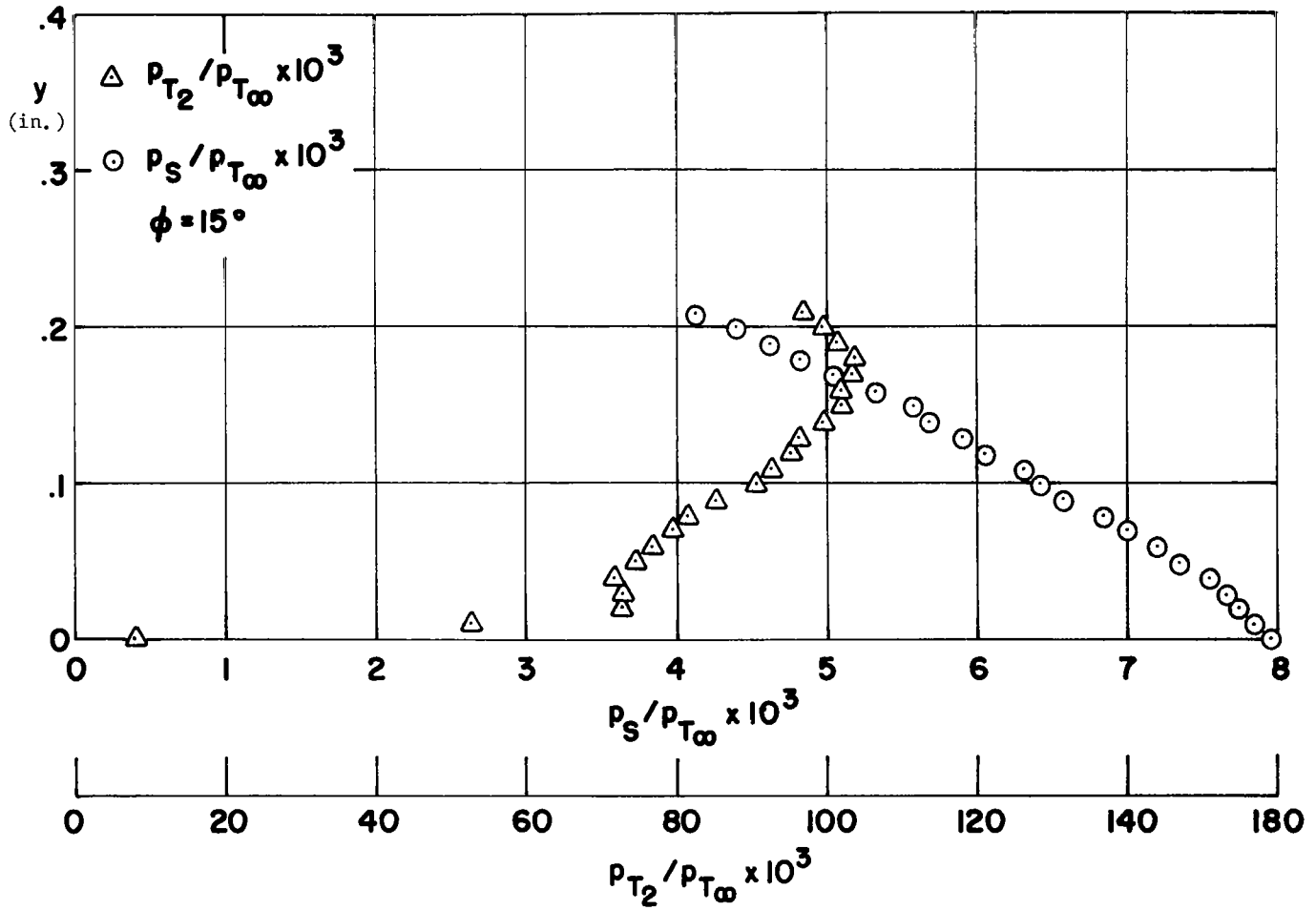

Fig. 9 Static and pitot pressure profiles

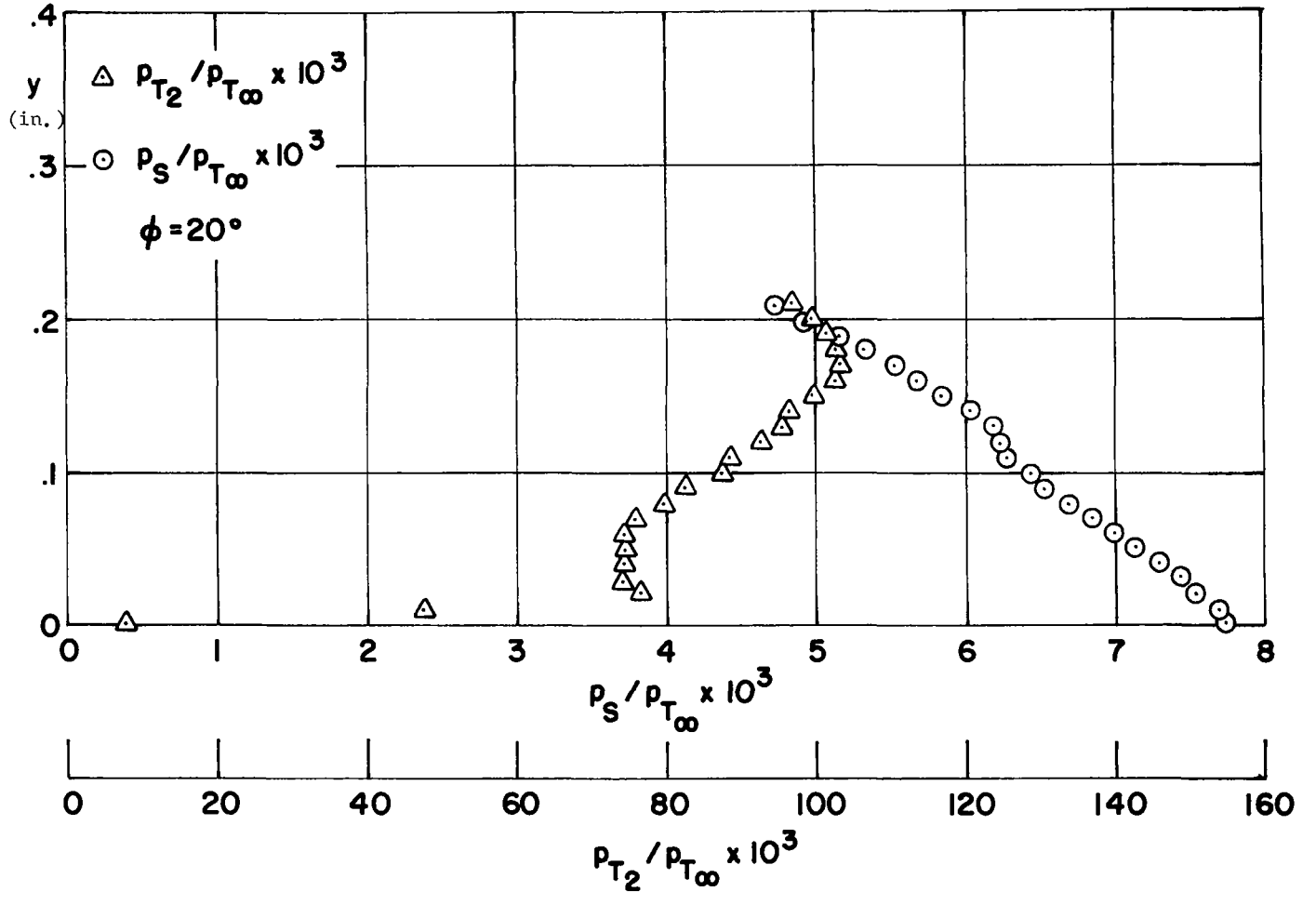

Fig. 10 Static and pitot pressure profiles

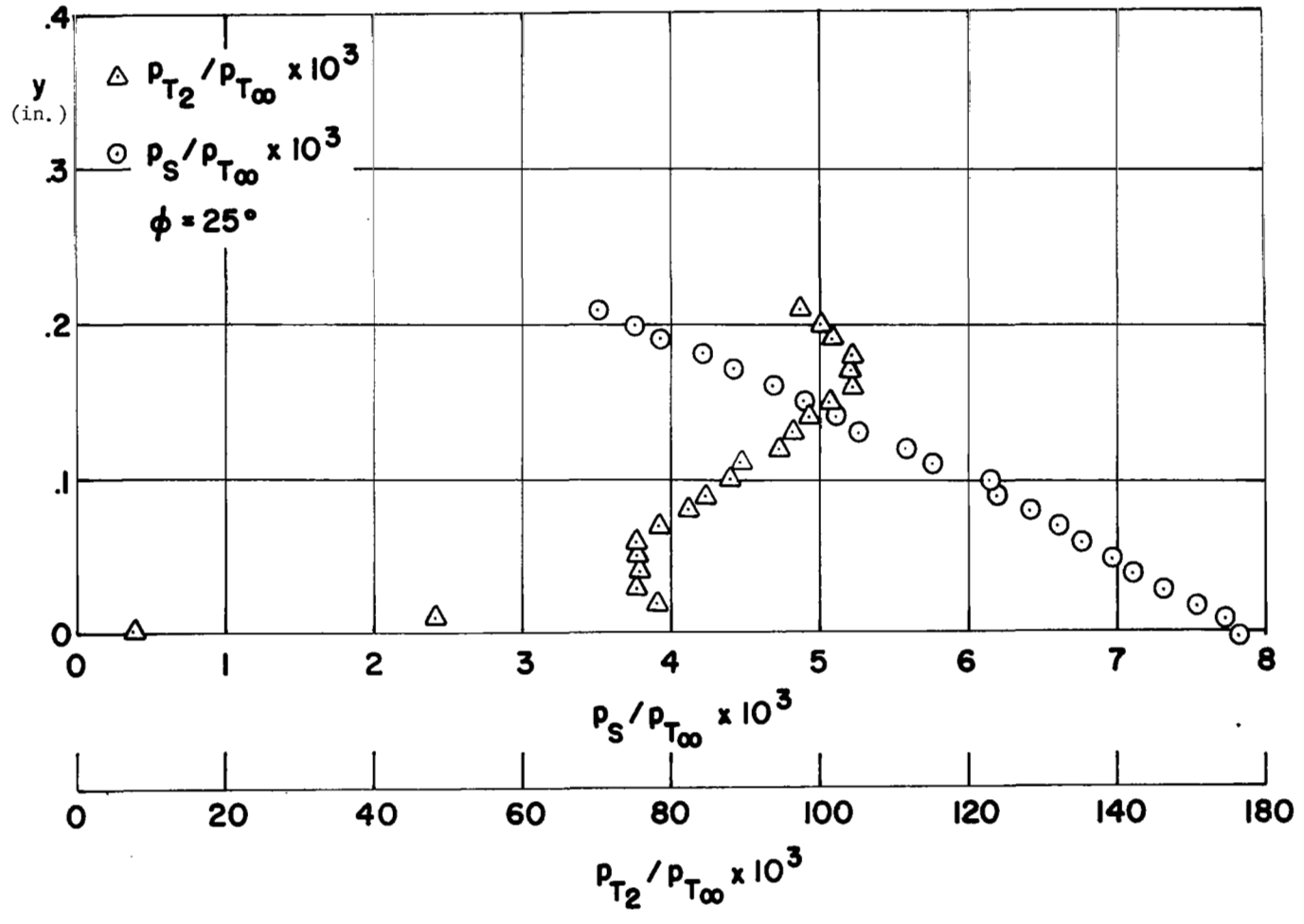

Fig. 11 Static and pitot pressure profiles

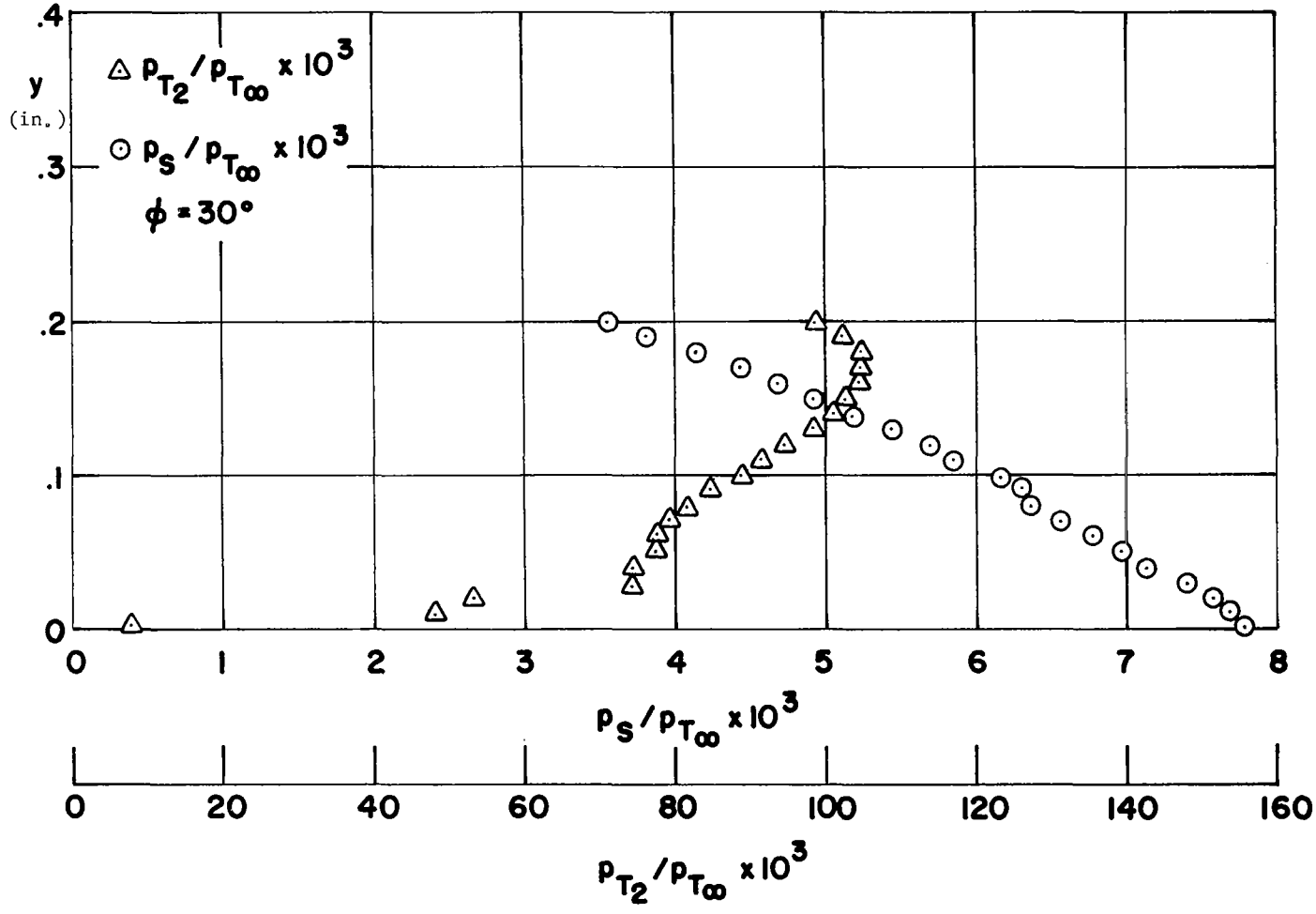

Fig. 12 Static and pitot pressure profiles

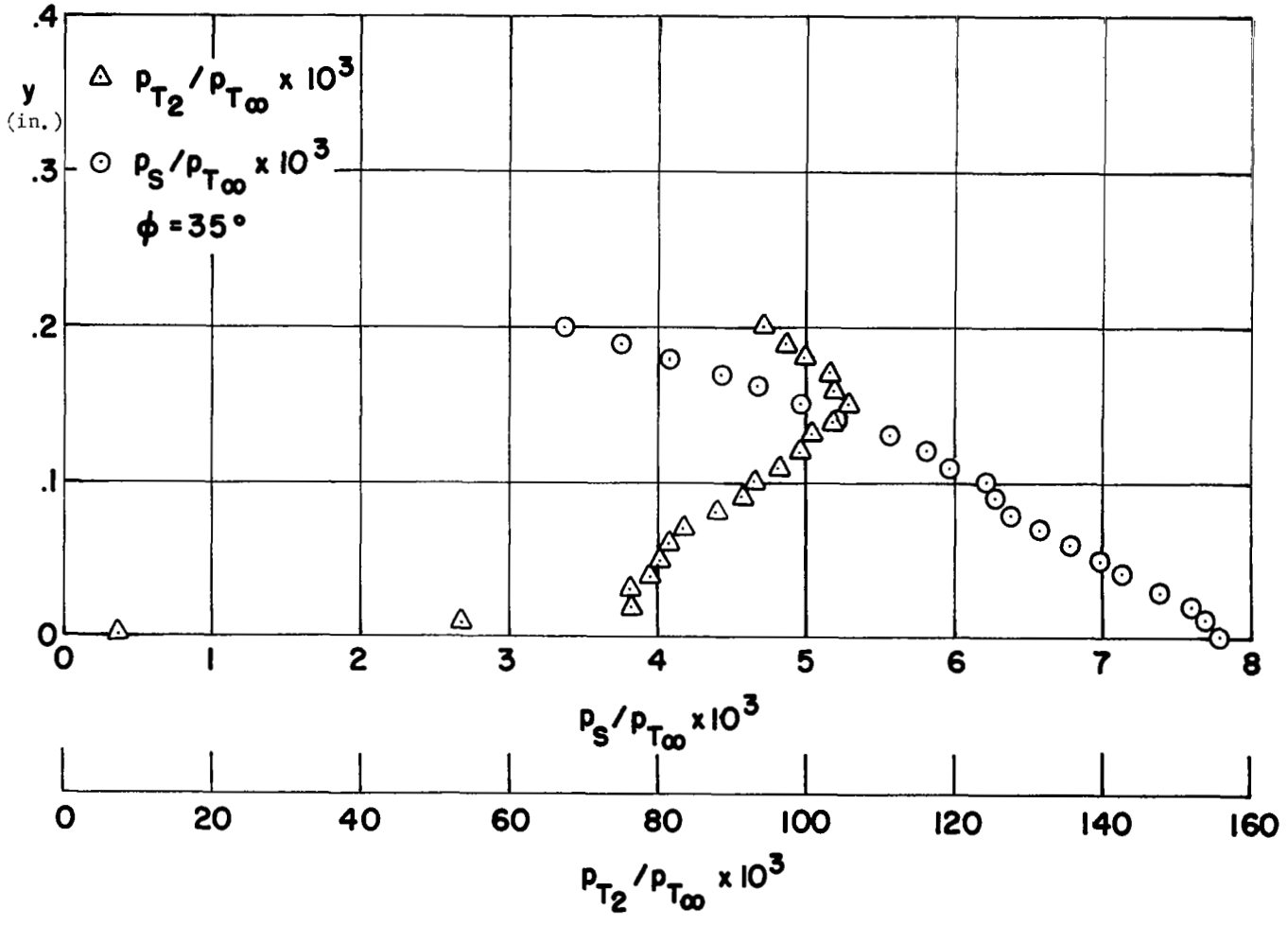

Fig. 13 Static and pitot pressure profiles

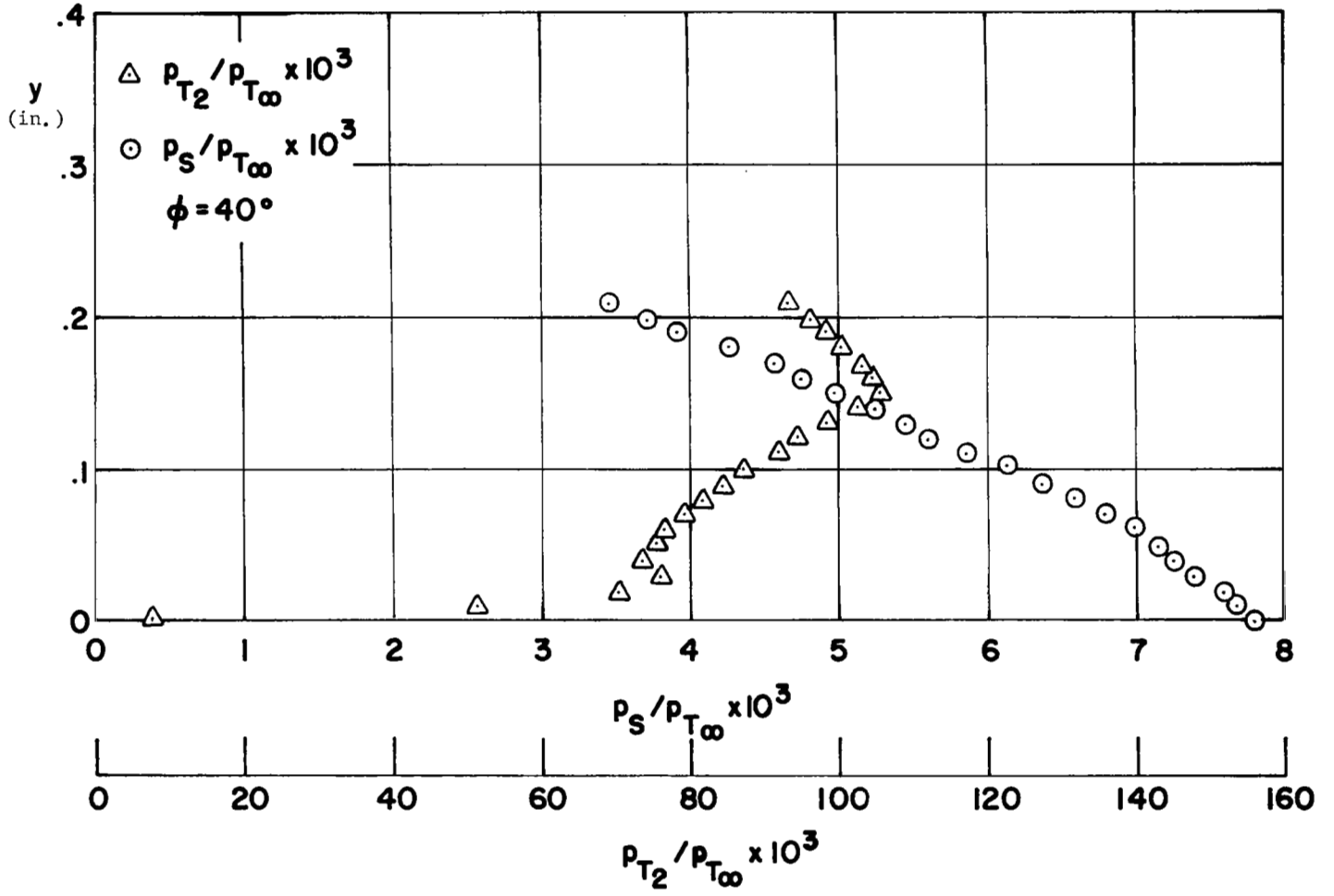

Fig. 14 Static and pitot pressure profiles

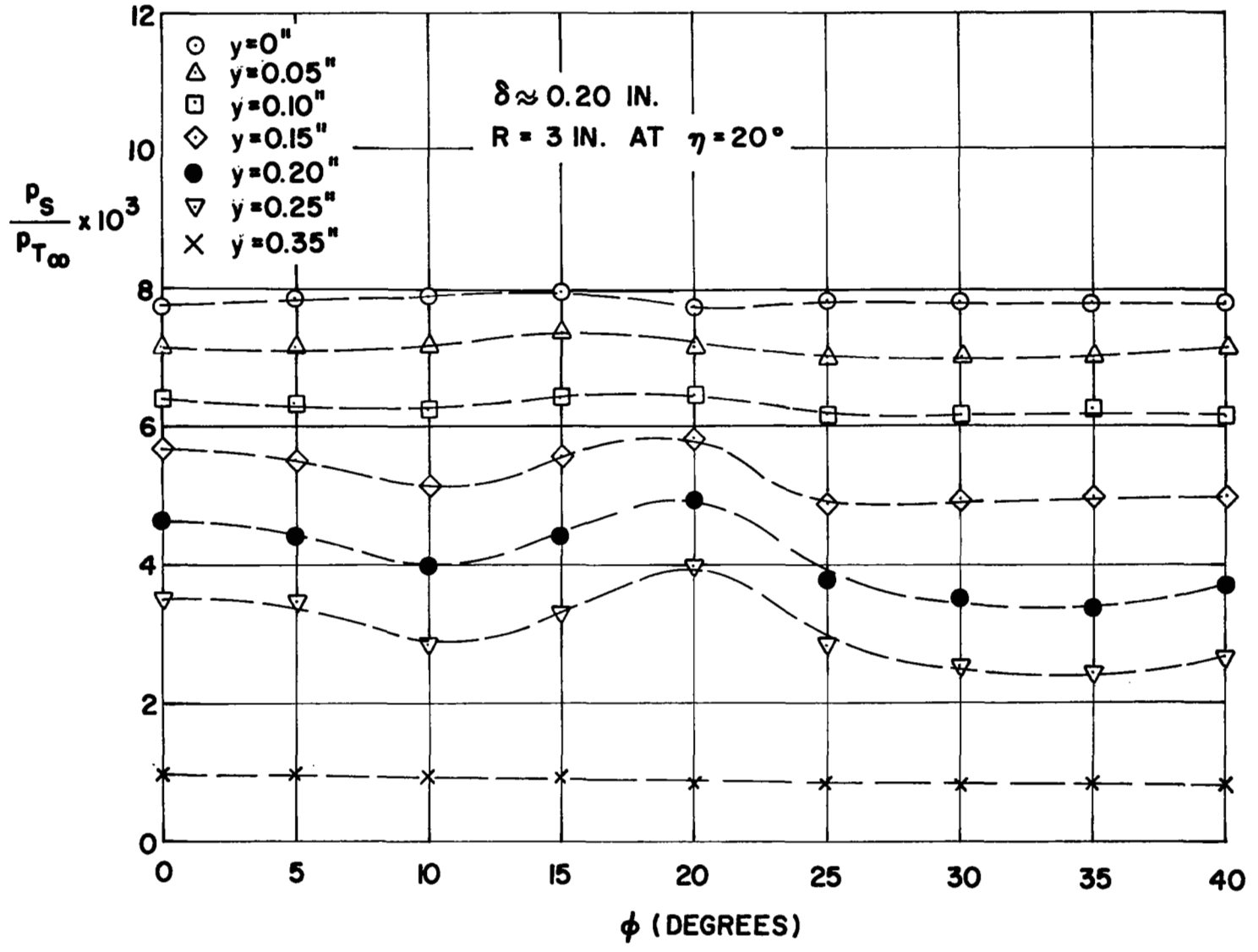

Fig. 15 Peripheral static pressure distribution

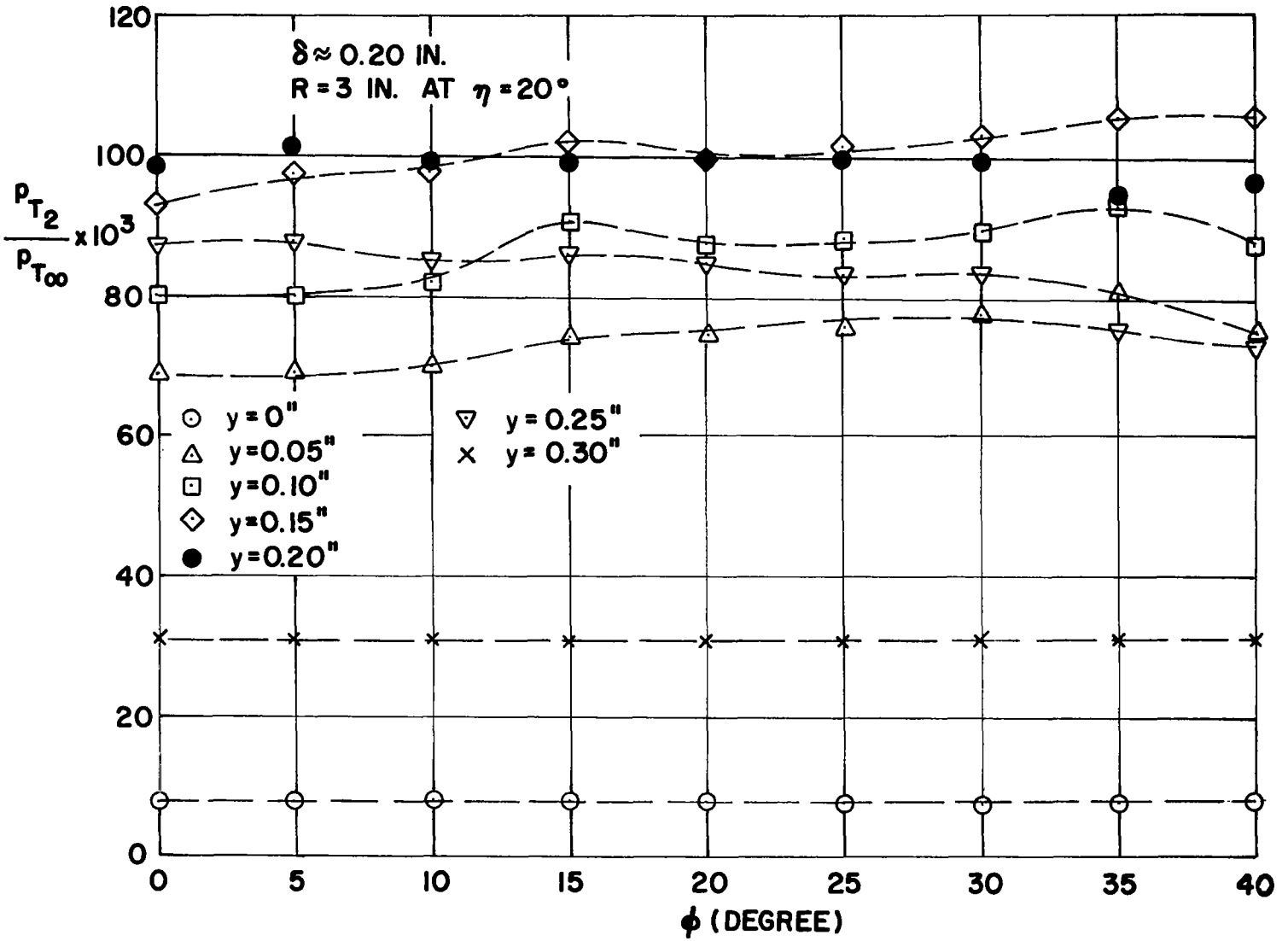

Fig. 16 Peripheral pitot pressure distribution

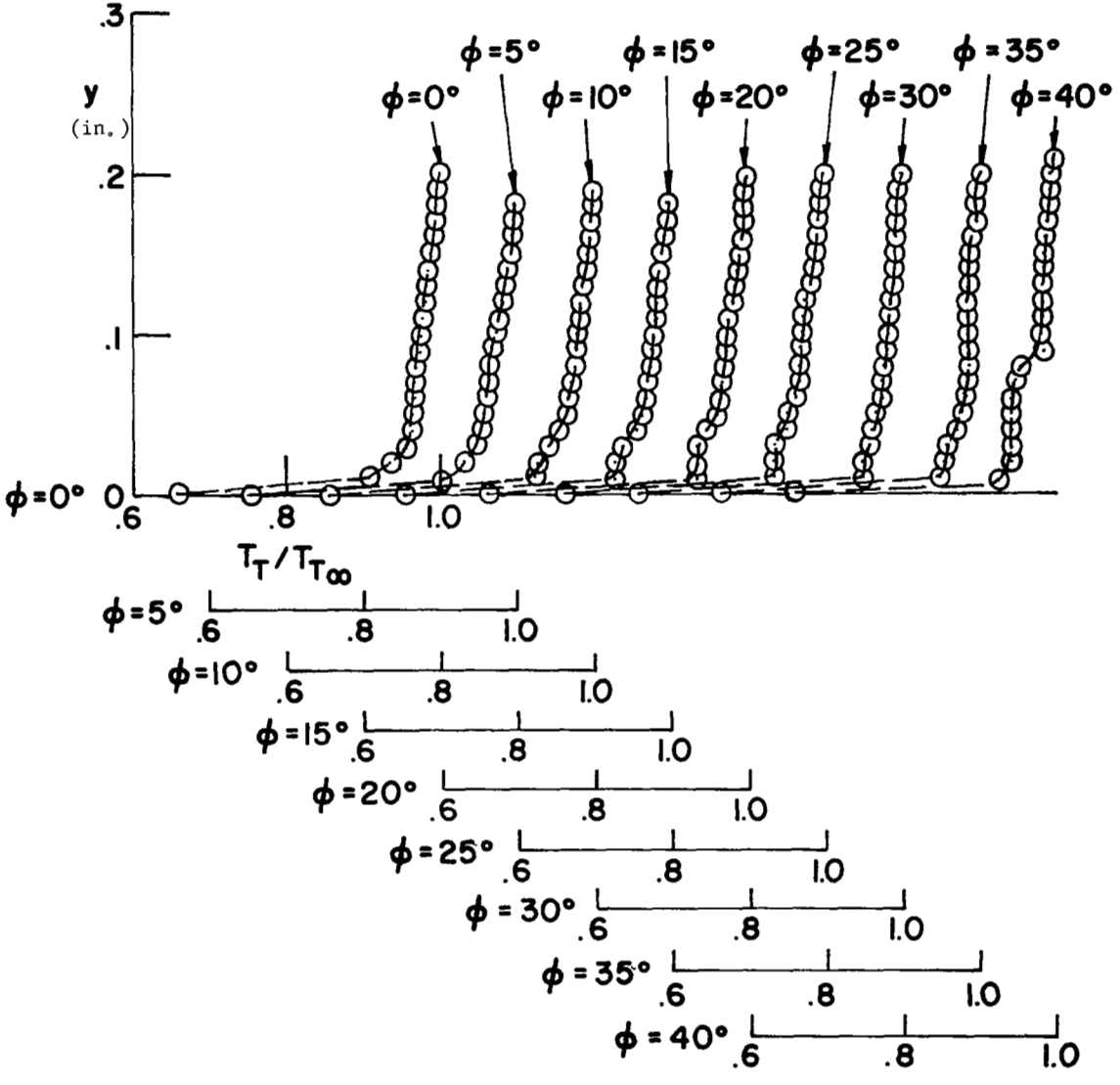

Fig. 17 Stagnation temperature profiles

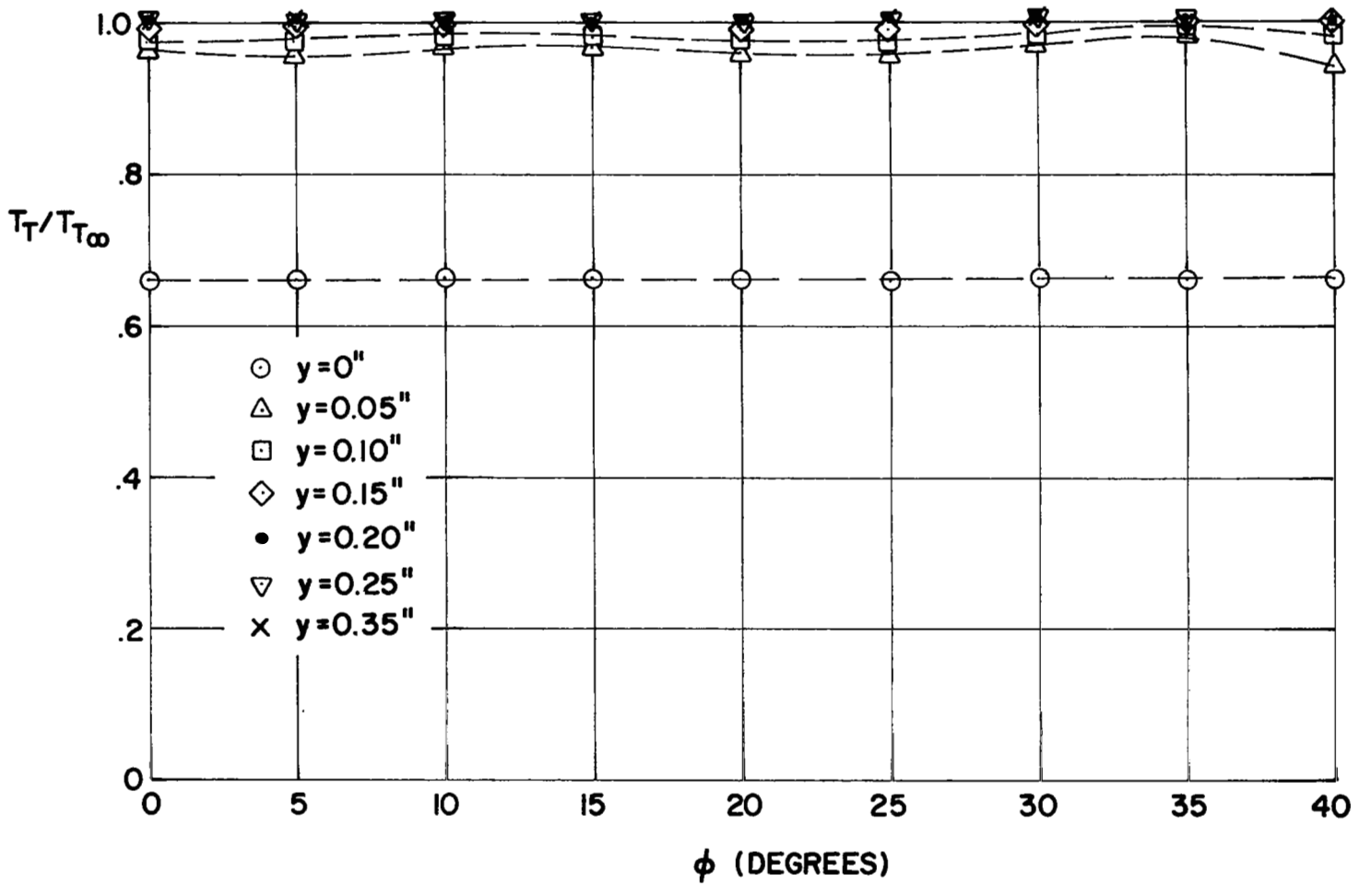

Fig. 18 Peripheral stagnation temperature distribution

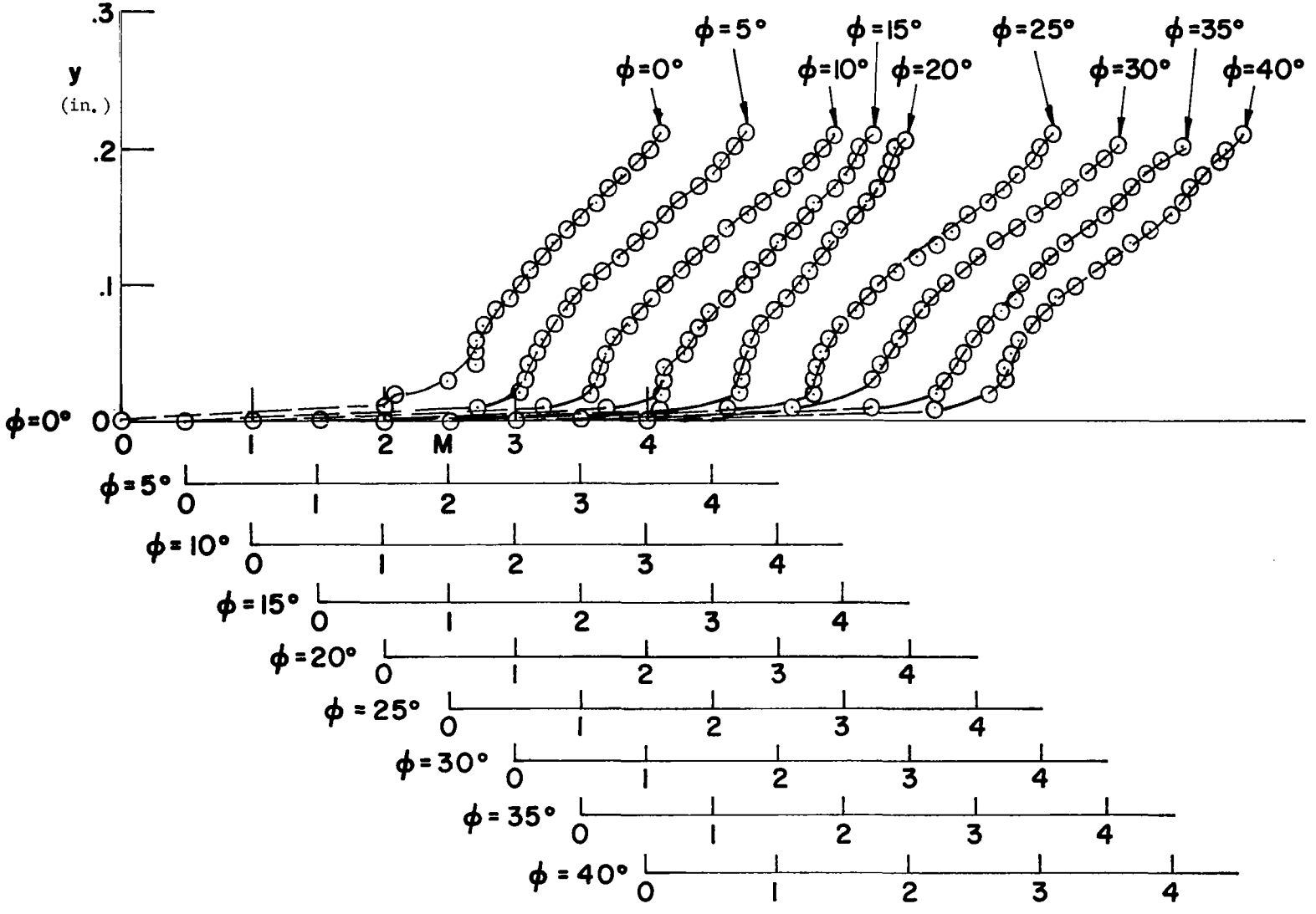

Fig. 19 Mach number profiles

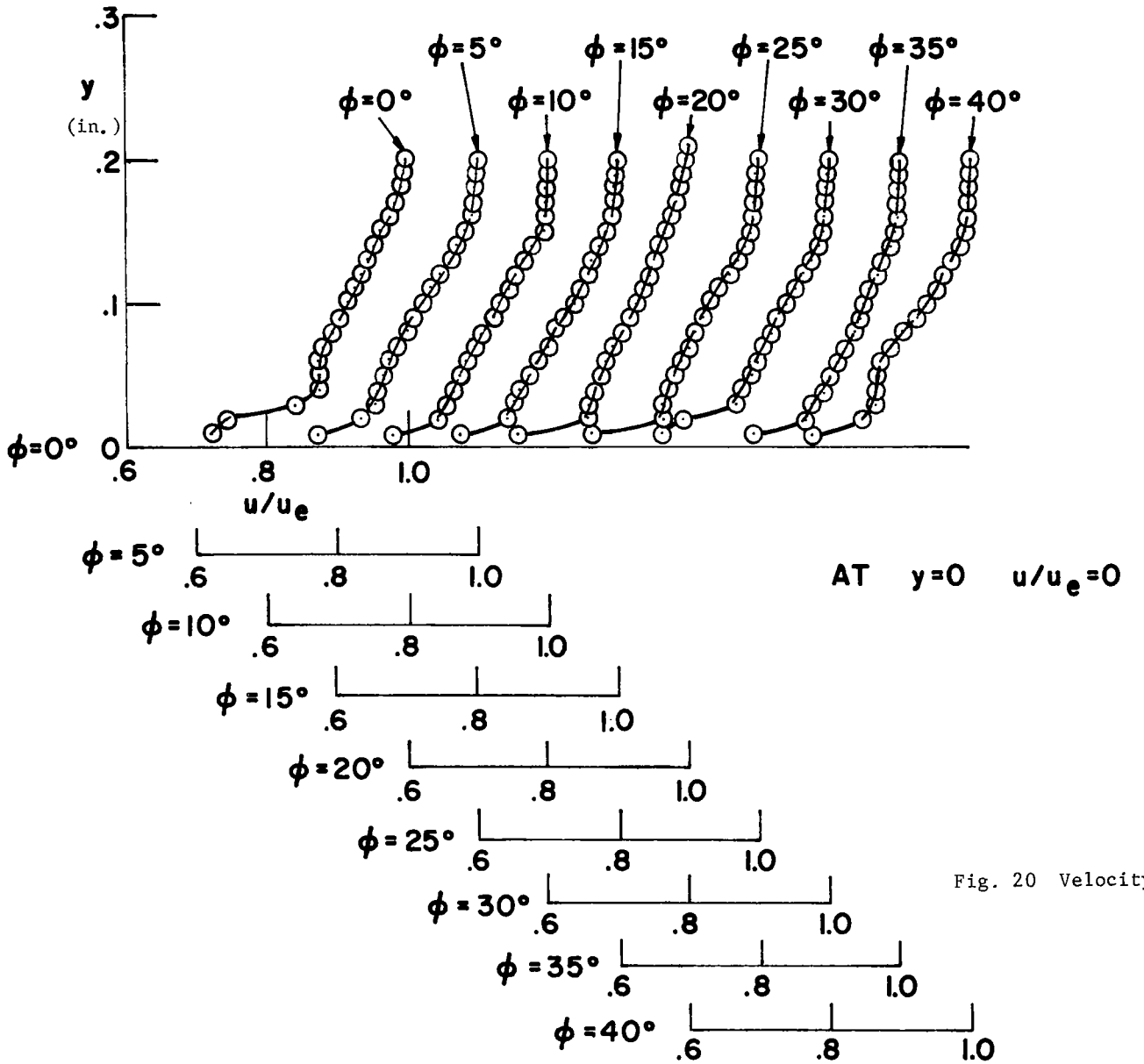

Fig. 20 Velocity profiles

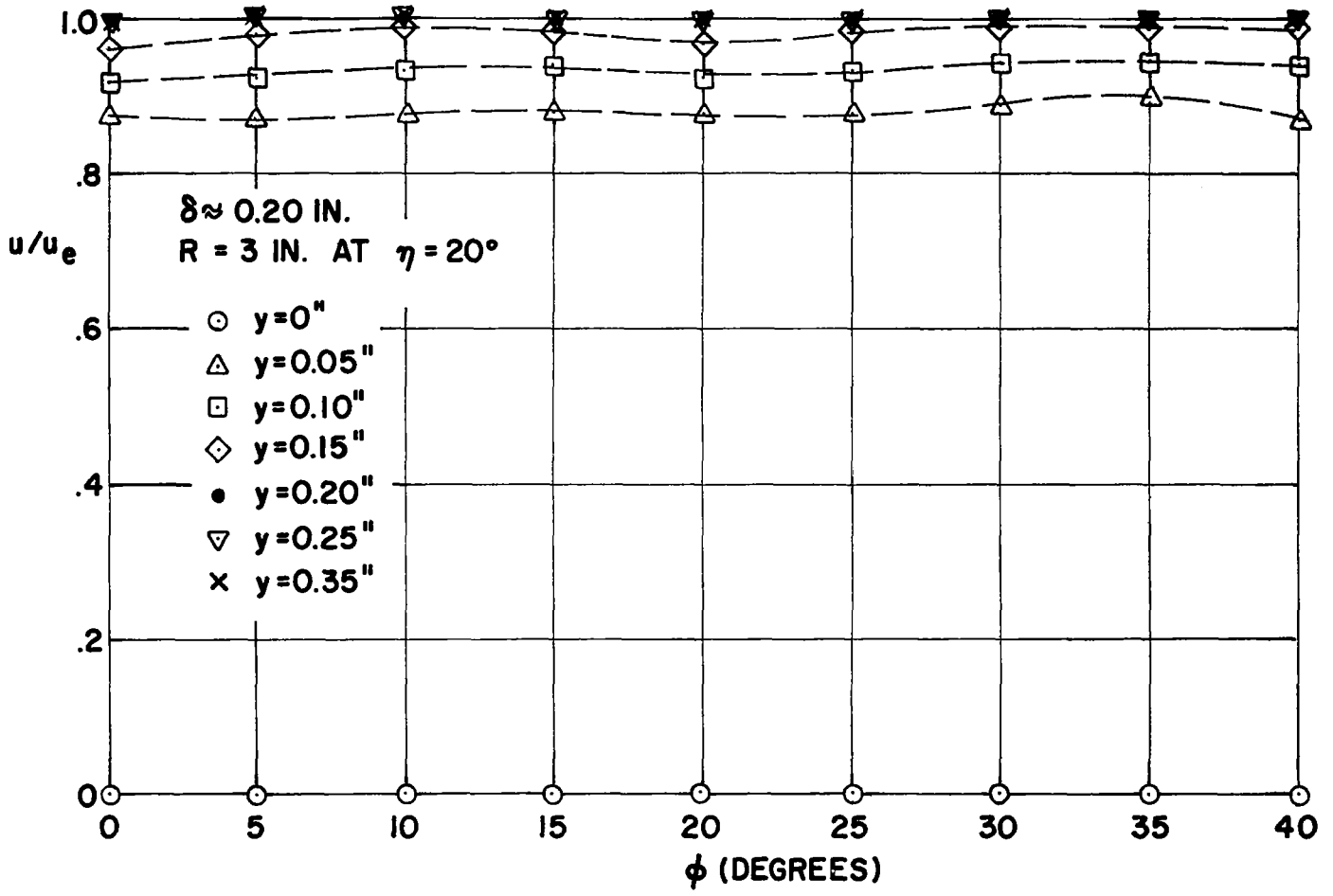

Fig. 21 Peripheral velocity distribution

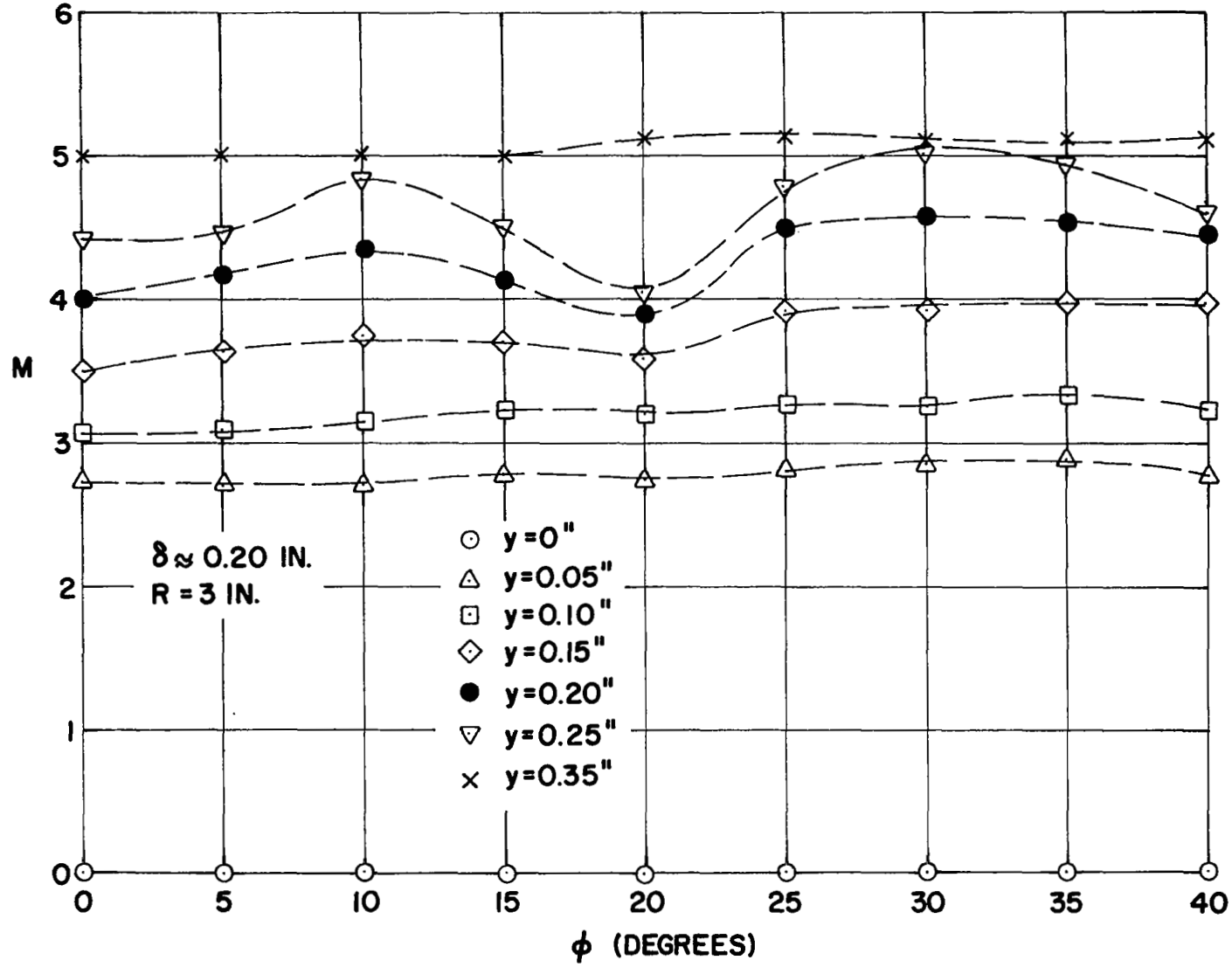

Fig. 22 Peripheral Mach number distribution